SLAC-PUB-2825
PEP-NOTE-371
October 1981
(A)

Particle Losses At Short Times After Injection*

S. Kheifets
M. Woodley
Stanford Linear Accelerator Center
Stanford, CA 94305

Summary

A transverse distribution of injected particles in a storage ring is often far from the equilibrium Gaussian distribution. In addition, the characteristic size of the injected bunch can be comparable with the aperture of the machine. This is especially true of positron injection. This situation occurs, for example, in the damping ring of the SLAC Single Pass Collider. In such cases one can expect particle losses. Questions now arise concerning the magnitude of these losses and their dependence on the ring parameters. We suggest here the answers to these questions for a one-dimensional particle motion.

(Submitted to Particle Accelerators)

* Work supported by the Department of Energy, Contract DE-AC03-76SF00515

1. Introduction

It is well known that in an electron storage ring the combined actions of radiation damping and quantum fluctuations bring particles to a stationary Gaussian distribution which can be expressed in the following manner:

Let τ_{rad} be the radiation damping time, and let D be the diffusion coefficient due to quantum fluctuations of particles having amplitude a. Then the stationary distribution $\Psi(a)$ is:

$$\Psi(a) = (1/2\pi\sigma^2)\exp(-a^2/2\sigma^2) \qquad (1)$$

where

$$\sigma^2 = D\tau_{rad}/2 \qquad (2)$$

It is also known that this result is an approximation, valid only in the absence of any boundary. The presence of vacuum chamber walls distorts this distribution, especially its tail. Note that this distribution has zero value only for infinitely large amplitude a; a real distribution function should become zero at the wall, allowing for the finite lifetime of the stored beam.

If the ratio of the vacuum chamber size A to the characteristic size of the bunch σ is large enough, only a small fraction of the total number of particles is in the distribution tails. In this case the presence of the wall distorts the distribution only slightly, and particle losses and the corresponding quantum lifetime τ can be found from the unperturbed stationary Gaussian distribution[1,2,3]:

$$\tau = \tau_{rad}(\sigma^2/A^2)\exp(a^2/2\sigma^2) \qquad (3)$$

where A is the maximum amplitude of particle oscillation, defined by the machine aperture.

A more exact solution of the problem is obtained in reference 4. The presence of the wall is taken into account in this work by imposing the zero boundary condition on the distribution function:

$$\Psi(A) = 0 \qquad (4)$$

The solution found in reference 4 is valid if the quantum lifetime τ is much larger than the radiation damping time τ_{rad}. In the limit $A/\sigma \gg 1$ the expression for τ reduces to formula (3). All of these solutions have one common drawback in that they essentially deal only with equilibrium distributions. Hence they are unable to start from some initial distribution and include into consideration the transition from it to an equilibrium distribution with the time course.

The general exact solution of the one-dimensional problem is

obtained in reference 5. In Section 2 we describe this solution, which is valid for any ratio of τ/τ_{rad}. Section 3 gives examples of numerical computations using the derived formulae.

2. Distribution Function and Particle Losses

We consider here the motion of a particle in a plane. The Fokker-Planck equation for this case which governs the behavior in time of the distribution function Ψ of the square of particle amplitude u has the following form[6,7]:

$$(\partial\Psi/\partial\theta) = u(\partial^2\Psi/\partial u^2) + (u+1)(\partial\Psi/\partial u) + \Psi \qquad (5)$$

where we introduce the dimensionless time variable θ:

$$\theta = 2t/\tau_{rad} \qquad (6)$$

and the dimensionless amplitude variable u:

$$u = a^2/D\tau_{rad} = a^2/2\sigma^2 \qquad (7)$$

which is the ratio of the square of the amplitude of the particle oscillation to the rms of the square of the amplitude calculated using the unperturbed distribution function (1). The distribution function $\Psi(\theta,u)$ at all times θ satisfies the boundary condition:

$$\Psi(\theta,\xi) = 0 \qquad (8)$$

with

$$\xi = A^2/2\sigma^2 \qquad (9)$$

where A is the maximum allowable amplitude of particle oscillation. Equation (8) is a consequence of the condition that all particles which reach the aperture of the machine are lost.

Let us count time θ from the moment of injection. Then at $\theta=0$ the distribution function should satisfy the initial condition:

$$\Psi(0,u) = \Psi_0(u) \qquad (10)$$

where $\Psi_0(u)$ is the distribution function in u of the injected particles.

The integral of $\Psi(\theta,u)$ gives the number of particles which are still in the machine at the moment θ. In particular at $\theta=0$ this integral gives the number of injected particles. It is convenient to normalize this distribution to 1:

$$\int_0^{\xi} \psi_0(u)\, du = 1 \tag{11}$$

Then the fraction of the total number of injected particles which stays in the machine until time θ is:

$$n(\theta) = \int_0^{\xi} \psi(\theta,u)\, du \tag{12}$$

and the portion of injected particles which is lost up to the moment θ is $1-n(\theta)$.

To solve equation (5) together with the initial (10) and boundary (8) conditions we expand $\psi(\theta,u)$ into the following series:

$$\psi(\theta,u) = \sum_{n=0}^{\infty} b_n \exp(-\kappa_n,\theta) f_n(u) \tag{13}$$

Here b_n and κ_n are constants which will be defined shortly. The functions $f_n(u)$ are the solutions of the following differential equation:

$$u f_n'' + (u+1) f_n' + (1+\kappa_n) f_n = 0 \tag{14}$$

To insure that the series in equation (13) satisfies condition (8) at all times θ each function $f_n(u)$ should satisfy its own boundary condition:

$$f_n(\xi) = 0 \tag{15}$$

It is easy to see that $f_n(u)$ can be defined in terms of a confluent hypergeometric function $F(-\kappa_n,1,u)$:

$$f_n(u) = \exp(-u) F(-\kappa_n,1,u) \tag{16}$$

Equation (15) implicitly defines the constants κ_n:

$$F(-\kappa_n,1,\xi) = 0 \tag{17}$$

We see from this expression that κ_n is uniquely determined by the quantity ξ from equation (9). For each given value of ξ equation (17), in respect to κ_n, has infinitely many roots. Fig. 1 illustrates the behavior of $F(-\kappa,1,\xi)$ as a function of κ for ξ=30. Fig. 2 shows the dependence of the first four roots, κ_0 through κ_3, on ξ. For large ξ the n-th root tends to the integer n. Hence for large ξ and for large θ all the terms in (13) but the zeroth decrease exponentially. In this case we have:

$$\psi(\theta,u) \simeq b_0 \exp(-\kappa_0\theta - u) F(-\kappa_0,1,u) \tag{18}$$

where

$$(1/\kappa_0) = Ei(\xi) - \ln(\xi) - 0.577 \qquad (19)$$

Function $Ei(\xi)$ here is an integral exponent[8]. For large ξ, $Ei(\xi) \simeq \exp(\xi)/\xi$ and we have as the result for the quantum lifetime:

$$\tau = \tau_{rad}\exp(\xi)/2\xi \qquad (20)$$

which after substitution of expression (9) coincides with equation (3).

For very small κ_0:

$$F(-\kappa_0,1,u) \simeq 1 - [Ei(u)-\ln(u)-0.577]/[Ei(\xi)-\ln(\xi)-0.577]$$

and the solution (18) coincides with the solution obtained in reference 4.

Let us return now to the general expression (18). We still have to determine the coefficients b_n. To do this we use the initial condition (10):

$$\psi_0(u) = \sum_{n=0}^{\infty} b_n \exp(-u) F(-\kappa_n,1,u) \qquad (21)$$

As shown in the Appendix, when weighted by the factor $\exp(-u)$ the functions $F(-\kappa_n,1,u)$ are orthogonal to each other on the interval $[0,\xi]$. By using this property we get:

$$b_n = \frac{\int_0^{\xi} \psi_0(u) F(-\kappa_n,1,u)\, du}{\int_0^{\xi} \exp(-u) F^2(-\kappa_n,1,u)\, du} \qquad (22)$$

So, finally, for the distribution function we have the following expression:

$$\psi(\theta,u) = \sum_{n=0}^{\infty} \exp(-\kappa_n\theta - u) F(-\kappa_n,1,u) \frac{\int_0^{\xi} \psi_0(u) F(-\kappa_n,1,u)\, du}{\int_0^{\xi} \exp(-u) F^2(-\kappa_n,1,u)\, du} \qquad (23)$$

The general expression for the fraction of the number of injected particles which stays in the storage ring until time θ is:

$$n(\theta) = \sum_{n=0}^{\infty} \exp(-\kappa_n\theta) \frac{\int_0^{\xi} \exp(-u)F(-\kappa_n,1,u)\,du \int_0^{\xi} \psi_0(u)F(-\kappa_n,1,u)\,du}{\int_0^{\xi} \exp(-u)F^2(-\kappa_n,1,u)\,du} \tag{24}$$

3. Numerical Results

In this section we describe the techniques and results of the computation of $n(\theta)$ and $\psi(\theta,u)$ for five different initial particle distributions.

I) Techniques:

In each case we compute an approximation of $n(\theta)$ by truncating the infinite series of (24) after an appropriate number of terms. Rewriting (24) we have:

$$n(\theta) \simeq \sum_{n=0}^{\bar{n}} b_n \exp(-\kappa_n\theta) \int_0^{\xi} \exp(-u)F(-\kappa_n,1,u)\,du \tag{25}$$

where $\bar{n}$ is chosen so that the total computing time in each case is less than 30 minutes. (It turns out that, in each case, $\bar{n}$ is 10 or 11 and that the magnitude of the first truncated term is less than 10^{-8}.)

Our program needs only to compute $n(\theta)$ for one particular value of θ; we used $\theta_0 = 1.0$. We compute $n(\theta')$ for any other time θ' in the following way:

$$N(\theta_0)_n \equiv b_n \exp(-\kappa_n\theta_0) \int_0^{\xi} \exp(-u)F(-\kappa_n,1,u)\,du \tag{26}$$

then

$$n(\theta_0) \simeq \sum_{n=0}^{\bar{n}} N(\theta_0)_n$$

and hence

$$n(\theta') \simeq \sum_{n=0}^{\bar{n}} \exp[-\kappa_n(\theta'-\theta_0)]N(\theta_0)_n \tag{27}$$

We begin our computation by generating a table of values of

$F(-\kappa,1,\xi)$ as a function of the parameter κ. The values from this table are shown plotted vs κ in fig. 1. We create this table by integrating the following differential equation subject to the given initial conditions (see equation (A1) in the Appendix):

$$\left.\begin{aligned} uF'' + (1-u)F' + \kappa F &= 0 \\ F(0) = 1 \;;\; F'(0) &= -\kappa \end{aligned}\right\} \qquad (28)$$

(note that we cannot integrate (28) to ξ starting at u=0; we actually integrate from $u=1.0\times10^{-10}$ without significant loss of precision).

We then use a simple bisection technique to find the zeros of the function of κ shown in fig. 1, thereby finding the values κ_n for which $F(-\kappa_n,1,\xi)$ satisfies the boundary condition (17). Using a standard numerical integration routine and the appropriate initial particle distribution function we then compute b_n from (22), and then $N(\theta_0)_n$ from (26); summation then yields $n(\theta_0)$.

Next, we generate plots of $n(\theta)$ vs θ by implementing (27) and finally, using the values of κ_n that we computed previously, we generate plots of $\Psi(\theta_{eq},u)$ by using (23). (θ_{eq} will be defined below...)

II) Results:

Our results are presented in the form of plots: $n(\theta)$ vs θ and $\Psi(\theta_{eq},u)$ for $0 < u < \xi$ where θ_{eq} is defined in such a way that the particle distribution function has reached equilibrium at some time $\theta < \theta_{eq}$; i.e. particle losses due to the transition from the initial particle distribution to the equilibrium distribution have occurred well before θ_{eq}. (We'll see that in all cases investigated particle losses due to this transition have pretty much died out by $\theta=1.0$; we used $\theta_{eq}=10$ to insure that equilibrium had been reached.) We performed our computations for five different initial particle distributions.

Initial Particle Distribution #1: $\Psi_0(u)$ Uniform in u:

This distribution function (uniform in the square of particle amplitude) has the form:

$$\Psi_0(u) = M \quad \text{for} \quad 0 \le u < \xi$$

where M is some constant. We normalize this distribution by implementing (11) and have for $\Psi_0(u)$:

$$\Psi_0(u) = 1/\xi$$

A plot of $n(\theta)$ vs θ ($\bar{n}=11$) for this initial distribution is shown in fig. 3. We note that the contributions from higher order terms in (27) decrease quickly and $n(\theta)$ rapidly approaches the value $N(\theta_0)_0$. For $\xi=30$, $\kappa_0 \simeq 10^{-11}$ which means that $n(\theta)$ decreases only very slowly after

the equilibrium particle distribution has been reached. For this particular initial distribution:

$$n(\theta) \simeq 0.9654 \quad \text{for} \quad \theta \geq \theta_{eq}$$

A comparison of the initial particle distribution with the equilibrium distribution for $\theta=\theta_{eq}$ is shown in fig. 4.

For the reader's further edification we present in fig. 5 a histogram plot of the relative magnitudes of the first 12 terms in the series of equation (26) for this initial particle distribution and $\xi=30$. We note some mathematically interesting behavior in the higher order terms, but only on a scale which is insignificant when compared to the zeroth order term which has a magnitude of order unity.

Initial Distribution #2: $\psi_0(u)$ Uniform in $\sqrt{u}$:

This distribution (uniform in particle amplitude) has the form:

$$\psi_0(\sqrt{u}) = M \quad \text{for} \quad 0 \leq u < \xi$$

As before, we normalize this distribution according to (11) and have for $\psi_0(u)$:

$$\psi_0(u) = (4\xi u)^{-1/2}$$

A plot of $n(\theta)$ vs θ ($\bar{n}=10$) for this initial distribution is shown in fig. 6. We see the same qualitative behavior that we saw in case #1; the initial decrease due to the transition to the equilibrium distribution is faster since the initial distribution is closer to the equilibrium distribution than in case #1. For our second initial distribution we have:

$$n(\theta) \simeq 0.9820 \quad \text{for} \quad \theta \geq \theta_{eq}$$

A comparison of the initial and equilibrium particle distributions for $\theta=\theta_{eq}$ is shown in fig. 7.

Initial Distributions #3,4,5: $\psi_0(u)$ Gaussian:

These distributions have the form:

$$\psi_0(u) = M \exp(-u^2/\sigma_0^2) \quad \text{for} \quad 0 \leq u < \xi$$

where $\sigma_0=\alpha\xi$; α is a parameter which determines the width of the initial Gaussian distribution. Normalizing in the usual manner using (11) we have for $\psi_0(u)$:

$$\psi_0(u) = [\sigma_0 C_\alpha]^{-1} \exp(-u^2/\sigma_0^2)$$

where

$$C_\alpha = \int_0^{1/\alpha} \exp(-x^2)\, dx$$

We consider now three different cases:

i) Narrow initial distribution ($\alpha=1/3$, $C_\alpha=0.8862$)

A plot of $n(\theta)$ vs θ ($\bar{n}=10$) for this initial distribution is shown in fig. 8. Again we see the same qualitative behavior that we've seen in the previous cases; the value of $n(\theta)$ after the transition to the equilibrium particle distribution is:

$$n(\theta) \simeq 0.9999 \quad \text{for} \quad \theta \geq \theta_{eq}$$

We note that for this case particle loss is quite small, since at all times the particles are far away from the boundary.

A comparison of the initial and equilibrium particle distributions for $\theta=\theta_{eq}$ is shown in fig. 9.

ii) Medium width initial distribution ($\alpha=1$, $C_\alpha=0.7468$)

A plot of $n(\theta)$ vs θ ($\bar{n}=11$) for this initial distribution is shown in fig. 10. The qualitative behavior of $n(\theta)$ for small θ is as seen previously; in this case $n(\theta)$ is:

$$n(\theta) \simeq 0.9818 \quad \text{for} \quad \theta \geq \theta_{eq}$$

A comparison of the initial and equilibrium particle distributions for $\theta=\theta_{eq}$ is shown in fig. 11.

iii) Broad initial distribution ($\alpha=3$, $C_\alpha=0.3214$)

A plot of $n(\theta)$ vs θ ($\bar{n}=11$) for this initial distribution is shown in fig. 12. The qualitative behavior for small θ is as before. For this case $n(\theta)$ is:

$$n(\theta) \simeq 0.9677 \quad \text{for} \quad \theta \geq \theta_{eq}$$

This value is smaller than in the previous two cases due to the increased width of the initial distribution.

A comparison of the initial and equilibrium particle distributions for $\theta=\theta_{eq}$ is shown in fig. 13.

Our final plot (fig. 14) illustrates the effect that the machine aperture parameter ξ has on the fraction of injected particles remaining in the beam at time θ_{eq}; i.e. the portion of the injected bunch remaining in the machine after the transition from the initial to the equilibrium distribution. For this plot we have used the broad Gaussian distribution ($\alpha=3$) as the initial particle distribution.

References

1. H. Bruck, Accelerateurs Circulaire de Particules, Press Universitaires de France, Paris, 1966

2. M. Sands, The Physics of Electron Storage Rings, SLAC-121, 1970

3. K. Robinson, CEA-69, December 1, 1958

4. A. Chao, SLAC-PUB-1884, February, 1977

5. S. Kheifets, "Pribory and Technika Experimenta", N5, 1960 (In Russian)

6. S. Chandrasekhar, "Rev. Mod. Phys", 15, 1 (1943)

7. L. Goldin, D. Koshkarev, "Nuovo Cim.", 6, 286 (1957)

8. I.S. Gradshteyn, I.M. Ryzhik, Tables of Integrals, Series and Products, Academic Press, 1980

Appendix

Orthogonality of the confluent hypergeometric functions

A confluent hypergeometric function $F(-\kappa_n,1,u)$ satisfies the following differential equation[8]:

$$uF'' + (1-u)F' + \kappa_n F = 0 \tag{A1}$$

It is easy to show that the function $f(u) = \exp(-u)F(-\kappa_n,1,u)$ satisfies a similar equation:

$$uf'' + (1+u)f' + (1+\kappa_m)f = 0 \tag{A2}$$

Let us multiply equation (A1) by f and equation (A2) by F and subtract the second equation thus obtained from the first. We get:

$$(\kappa_m-\kappa_n)fF = d[u(fF'-f'F-fF)]/du \tag{A3}$$

Now we integrate both sides of equation (A3) over u from 0 to ξ. Each of the functions f and F satisfies its own boundary condition:

$$F(-\kappa_n,1,\xi) = 0 \tag{A4}$$

$$f(-\kappa_m,1,\xi) = 0 \tag{A5}$$

Hence, by integrating (A3) one gets:

$$(\kappa_m-\kappa_n)\int_0^{\xi} fF\ du = 0 \tag{A6}$$

or

$$\int_0^{\xi} \exp(-u)F(-\kappa_m,1,u)F(-\kappa_n,1,u)\ du = N_n\delta_{n,m} \tag{A7}$$

where $\delta_{n,m}$ is the Kroneker symbol:

$$\delta_{n,m} = \begin{cases} 1 \text{ if } n=m \\ 0 \text{ if } n\neq m \end{cases} \tag{A8}$$

and N_n is some constant.

List of figure captions

Fig. 1 : $F(-\kappa,1,\xi)$ vs κ for $\xi=30$

Fig. 2 : κ_n vs ξ for $n=0,1,2,3$

Fig. 3 : $n(\theta)$ (sum of first 12 terms) vs θ for $\psi_0(u)$ uniform in u, $\xi=30$

Fig. 4 : Initial and final particle distributions: $\psi_0(u)$ (broken line) and $\psi(\theta_{eq},u)$ (solid line) for $\psi_0(u)$ uniform in u, $\xi=30$

Fig. 5 : Relative magnitudes of first 12 terms of $n(\theta)$ for $\psi_0(u)$ uniform in u, $\xi=30$ and $\theta=\theta_0=1.0$

Fig. 6 : $n(\theta)$ (sum of first 11 terms) vs θ for $\psi_0(u)$ uniform in $\sqrt{u}$, $\xi=30$

Fig. 7 : Initial and final particle distributions: $\psi_0(u)$ (broken line) and $\psi(\theta_{eq},u)$ (solid line) for $\psi_0(u)$ uniform in $\sqrt{u}$, $\xi=30$

Fig. 8 : $n(\theta)$ (sum of first 11 terms) vs θ for $\psi_0(u)$ narrow Gaussian ($\alpha=1/3$), $\xi=30$

Fig. 9 : Initial and final particle distributions: $\psi_0(u)$ (broken line) and $\psi(\theta_{eq},u)$ (solid line) for $\psi_0(u)$ narrow Gaussian ($\alpha=1/3$), $\xi=30$

Fig. 10 : $n(\theta)$ (sum of first 12 terms) vs θ for $\psi_0(u)$ medium width Gaussian ($\alpha=1$), $\xi=30$

Fig. 11 : Initial and final particle distributions: $\psi_0(u)$ (broken line) and $\psi(\theta_{eq},u)$ (solid line) for $\psi_0(u)$ medium width Gaussian ($\alpha=1$), $\xi=30$

Fig. 12 : $n(\theta)$ (sum of first 12 terms) vs θ for $\psi_0(u)$ broad Gaussian ($\alpha=3$), $\xi=30$

Fig. 13 : Initial and final particle distributions: $\psi_0(u)$ (broken line) and $\psi(\theta_{eq},u)$ (solid line) for $\psi_0(u)$ broad Gaussian ($\alpha=3$), $\xi=30$

Fig. 14 : Fraction of the number of injected particles remaining in the machine after the transition from the initial particle distribution to the equilibrium distribution as a function of the machine aperture parameter ξ

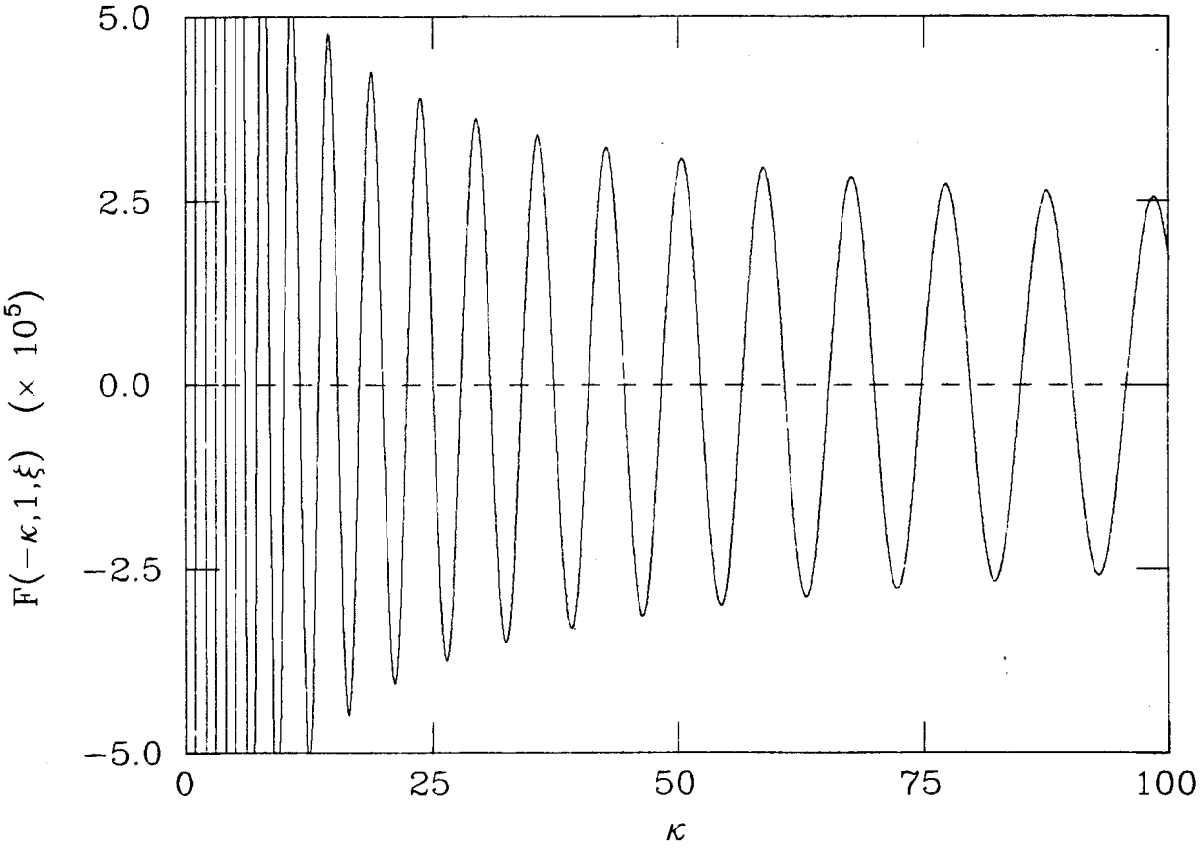

Fig. 1

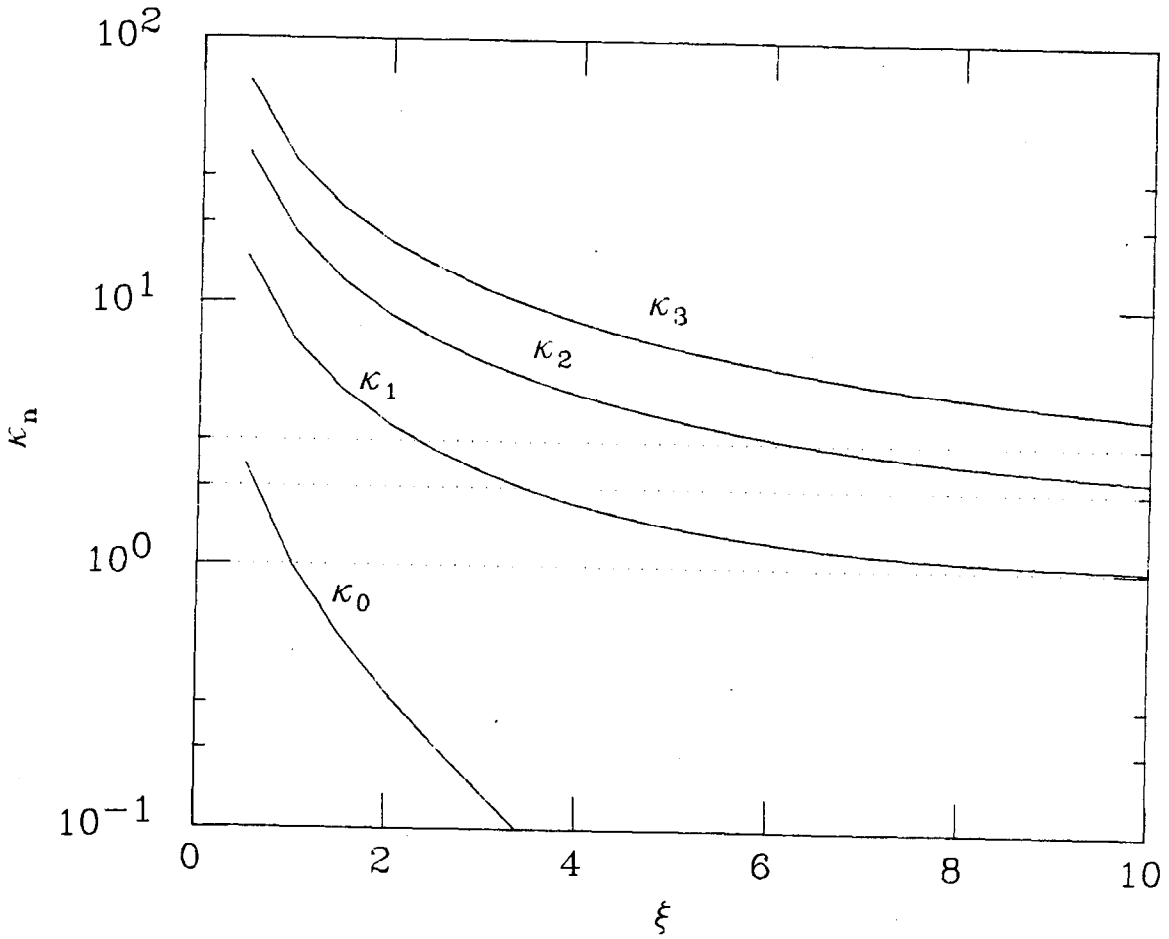
10^2
10^1
10^0
10^{-1}
κ_n
κ_3
κ_2
κ_1
κ_0
0
2
4
6
8
10
ξ

Fig. 2

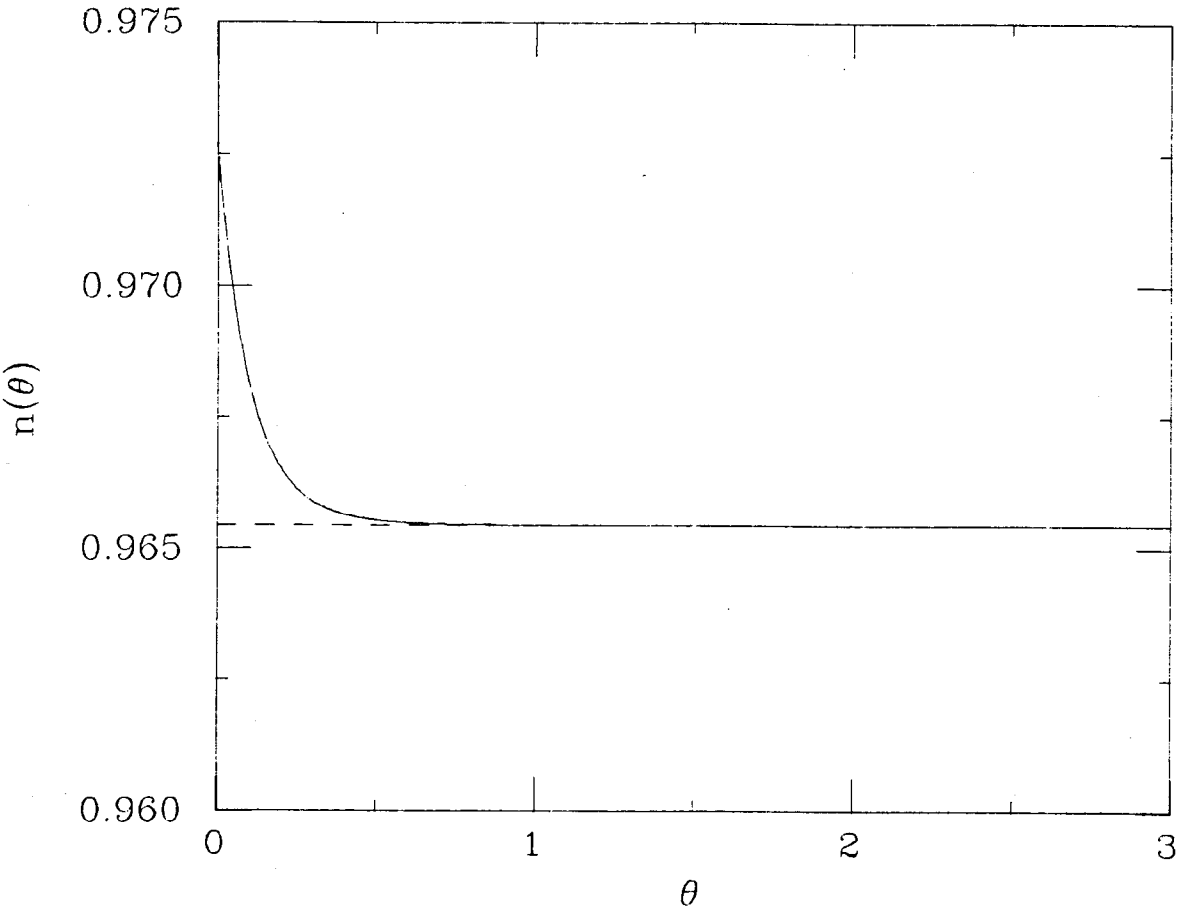

Fig. 3

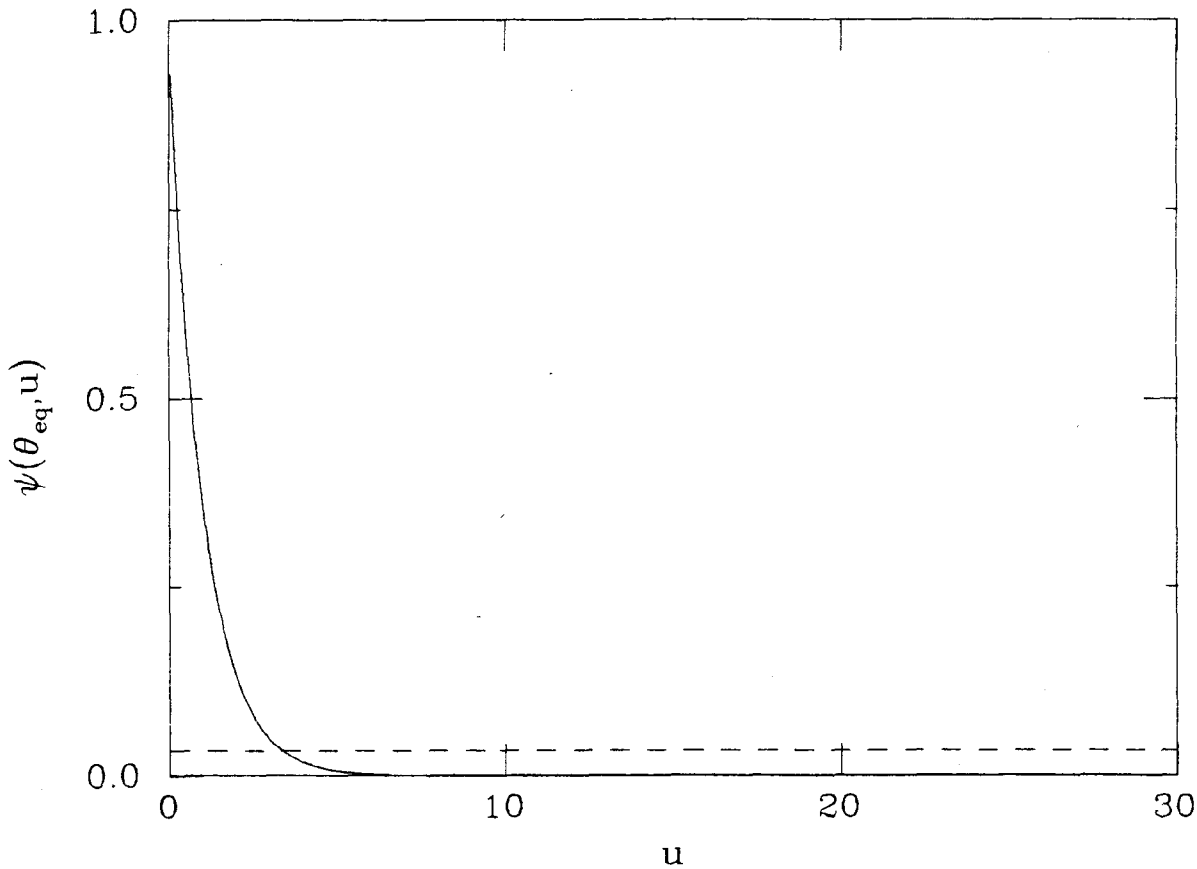

Fig. 4

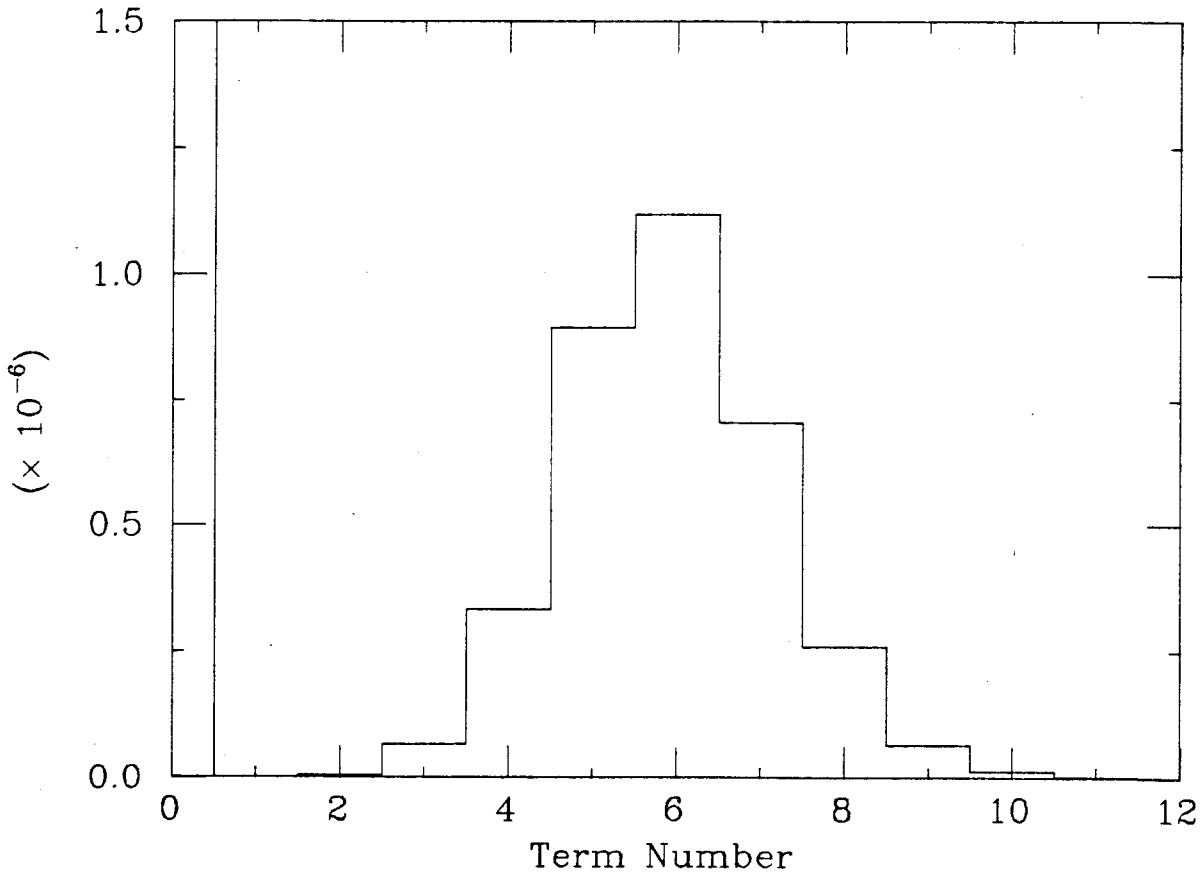

Fig. 5

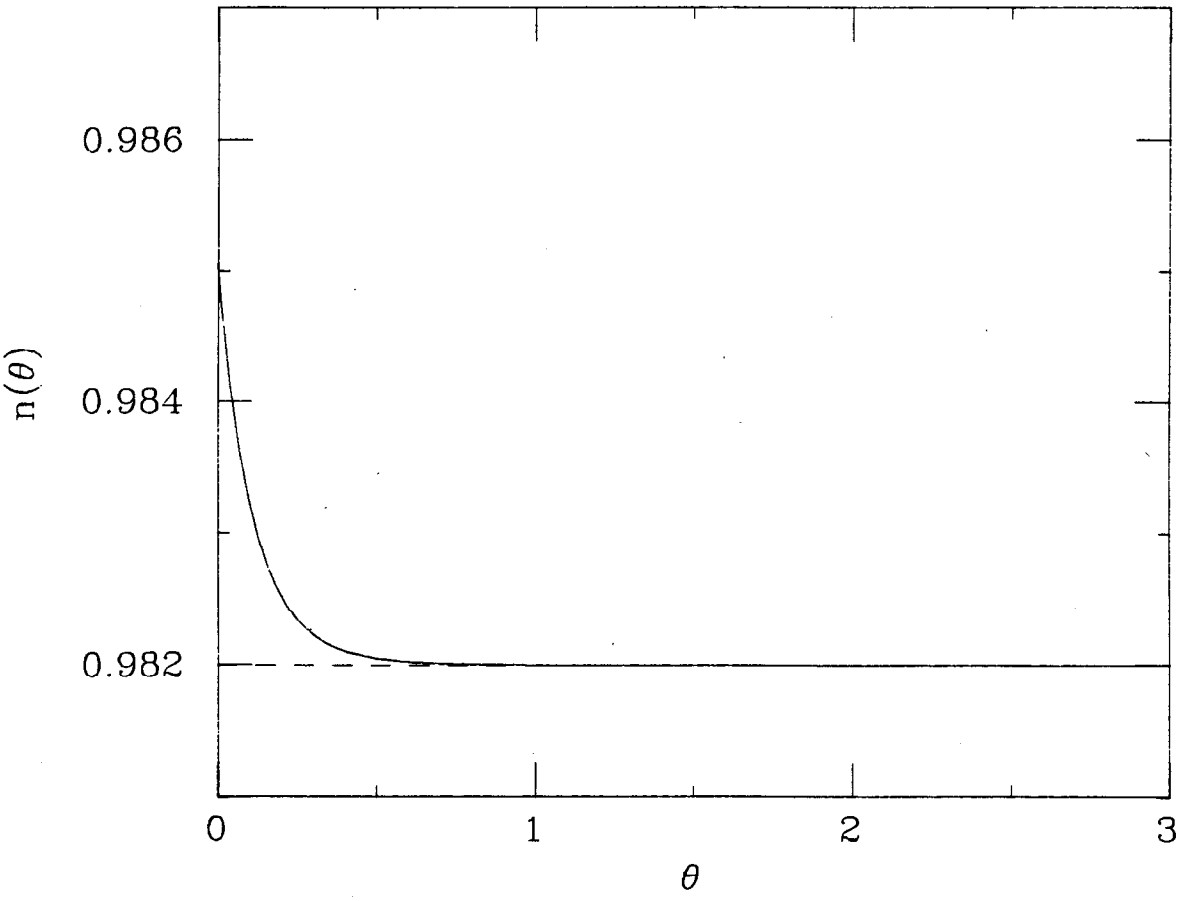

Fig. 6

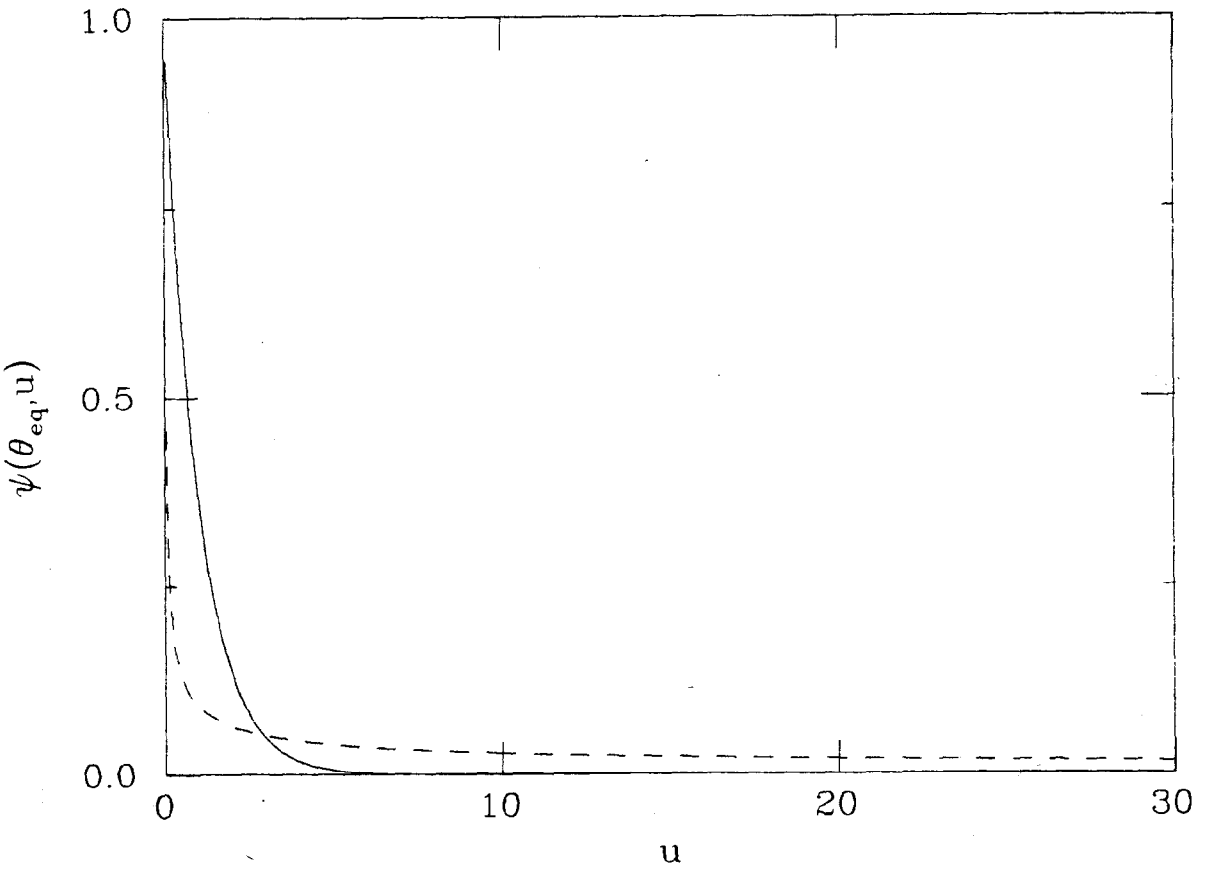

Fig. 7

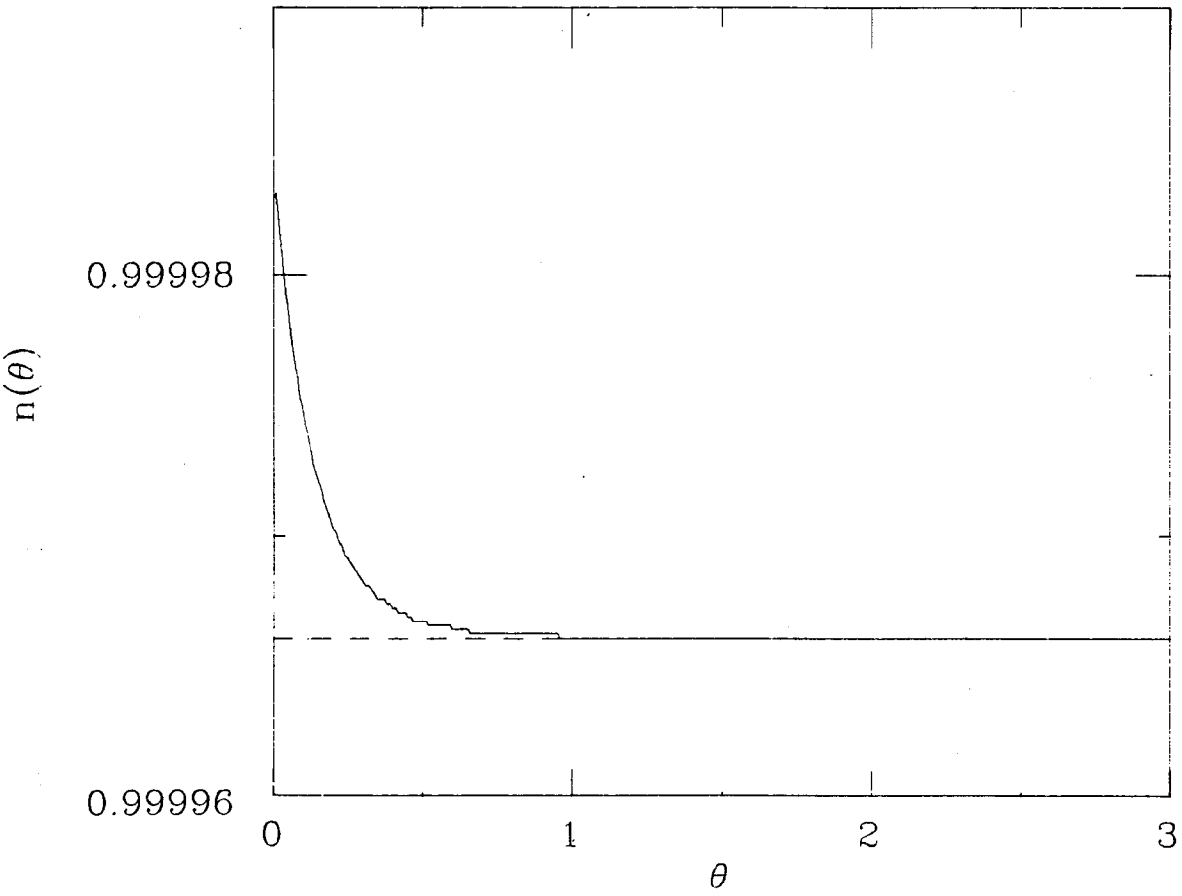

Fig. 8

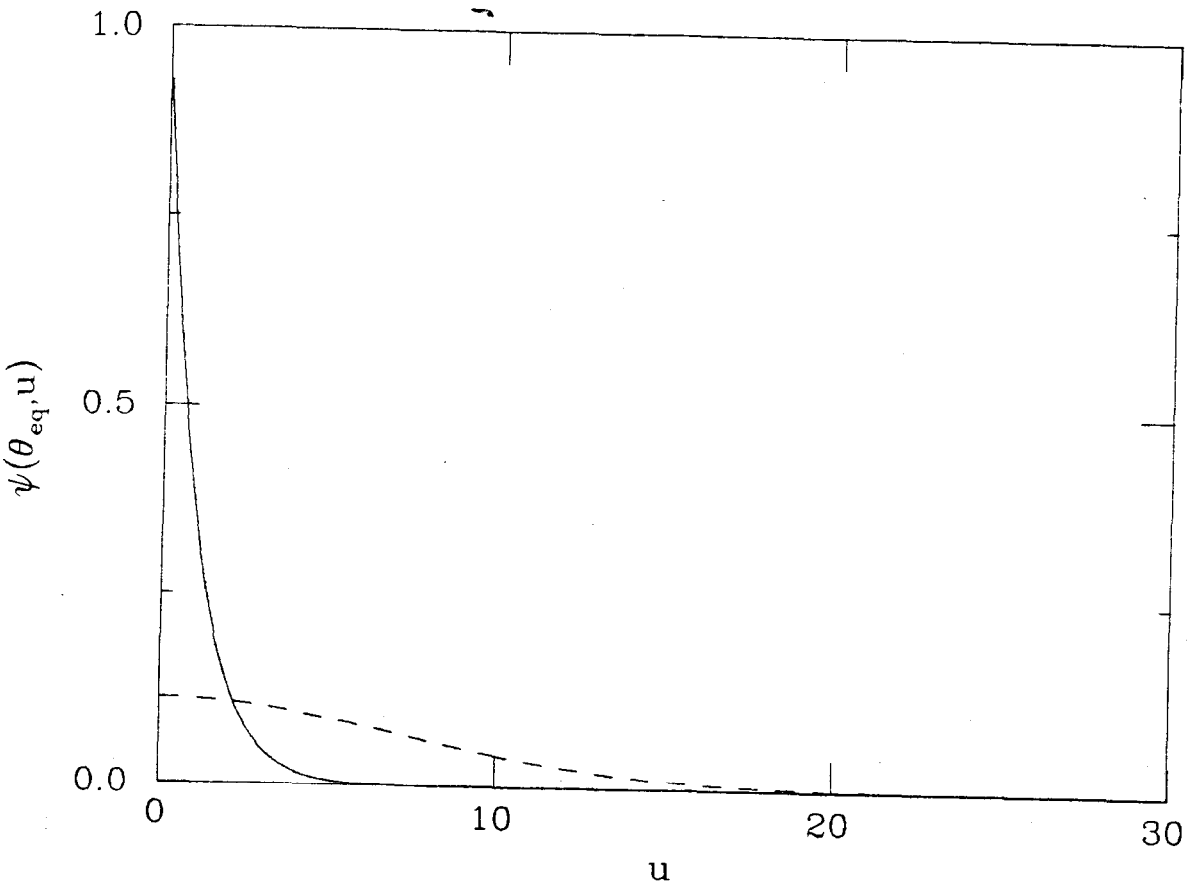

Fig. 9

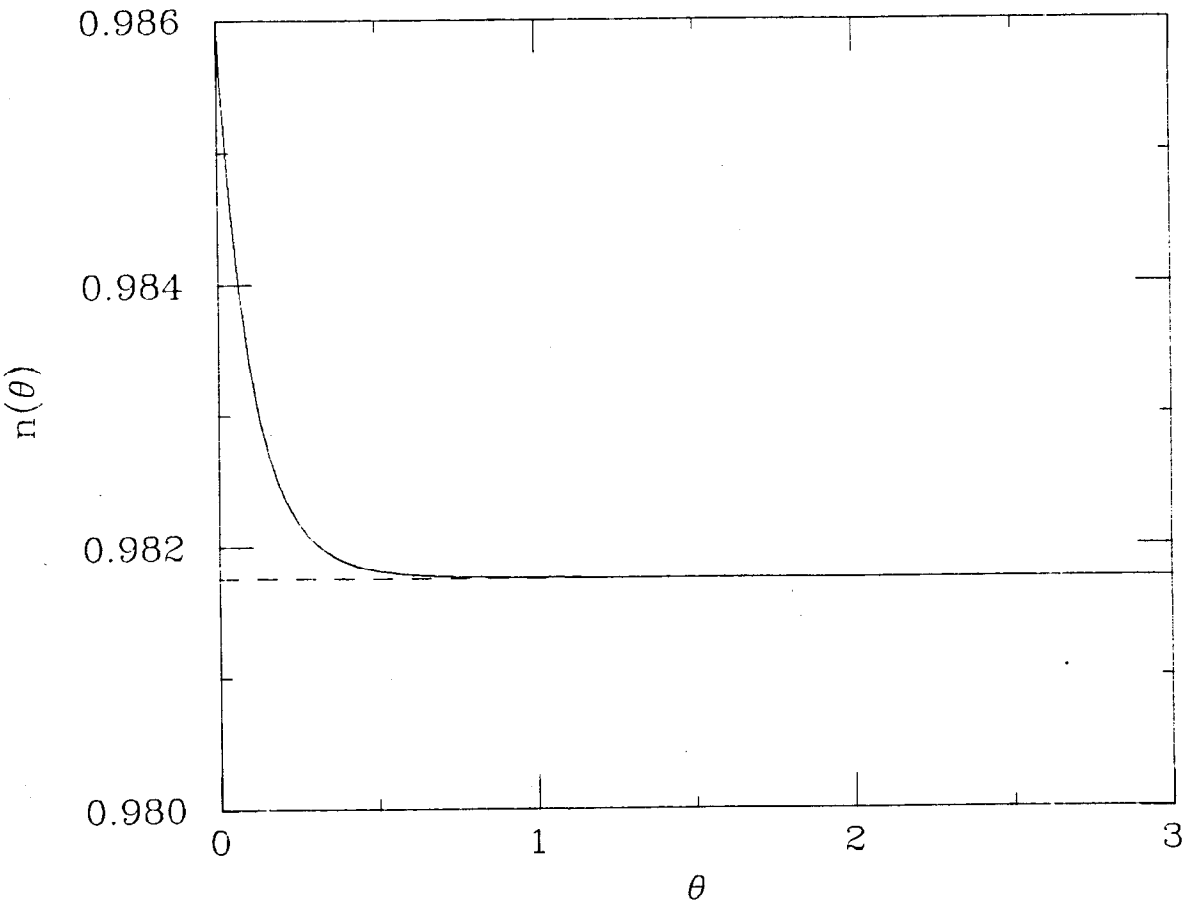

Fig. 10

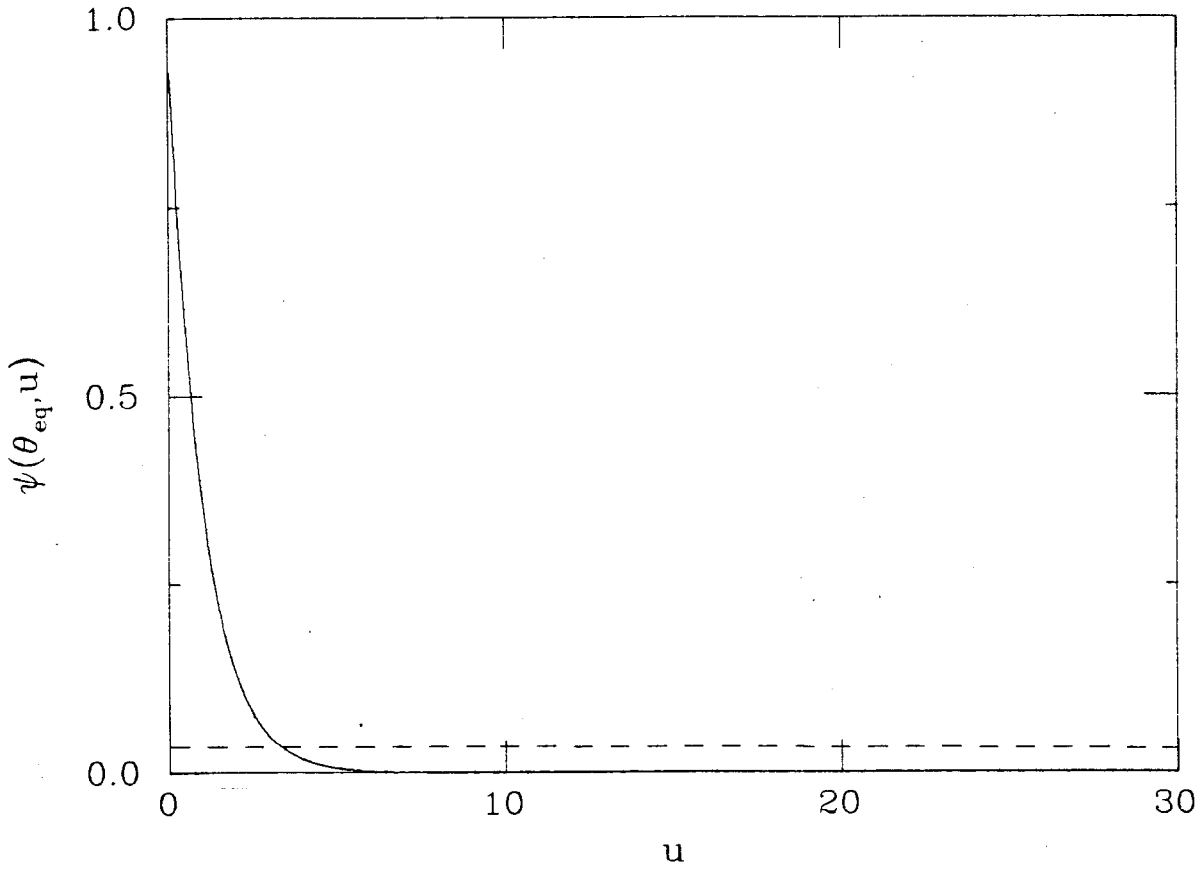

Fig. 11

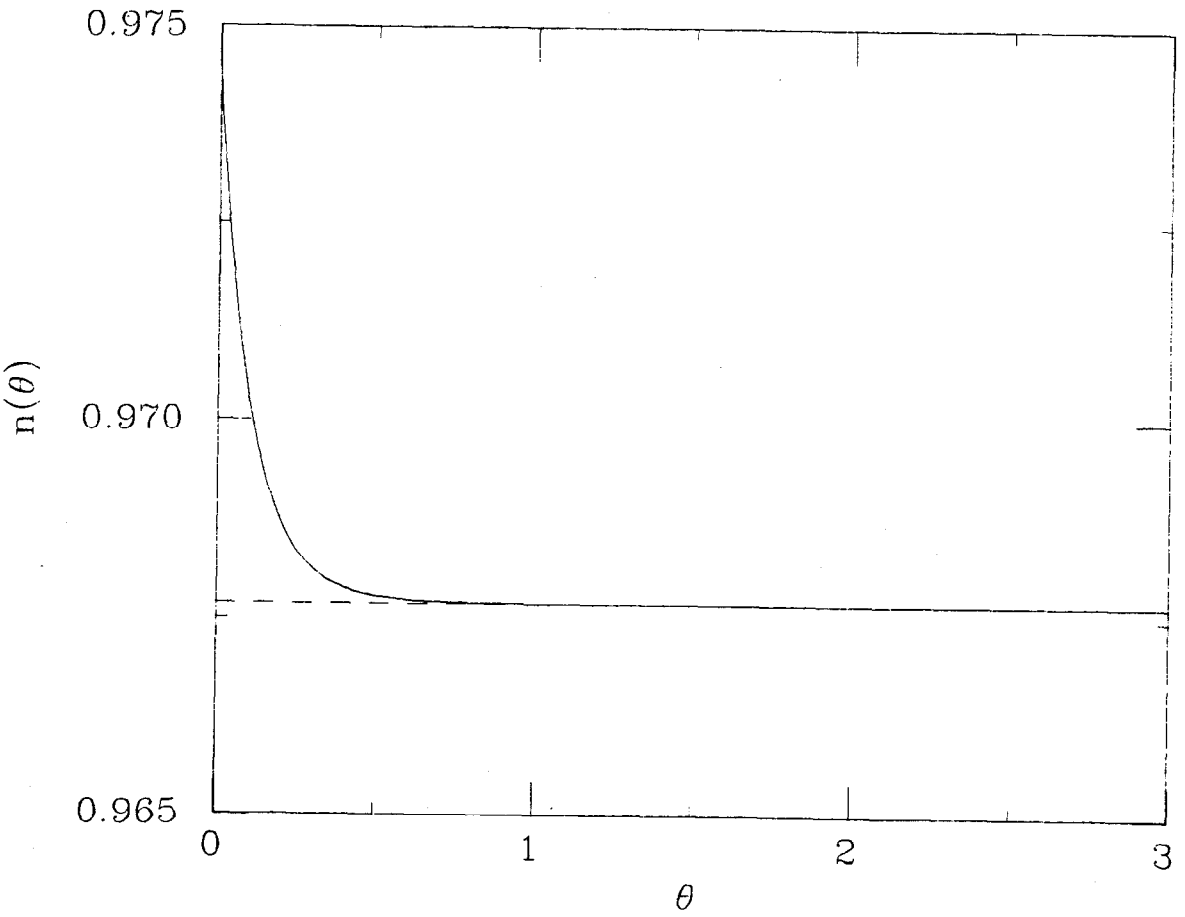

Fig. 12

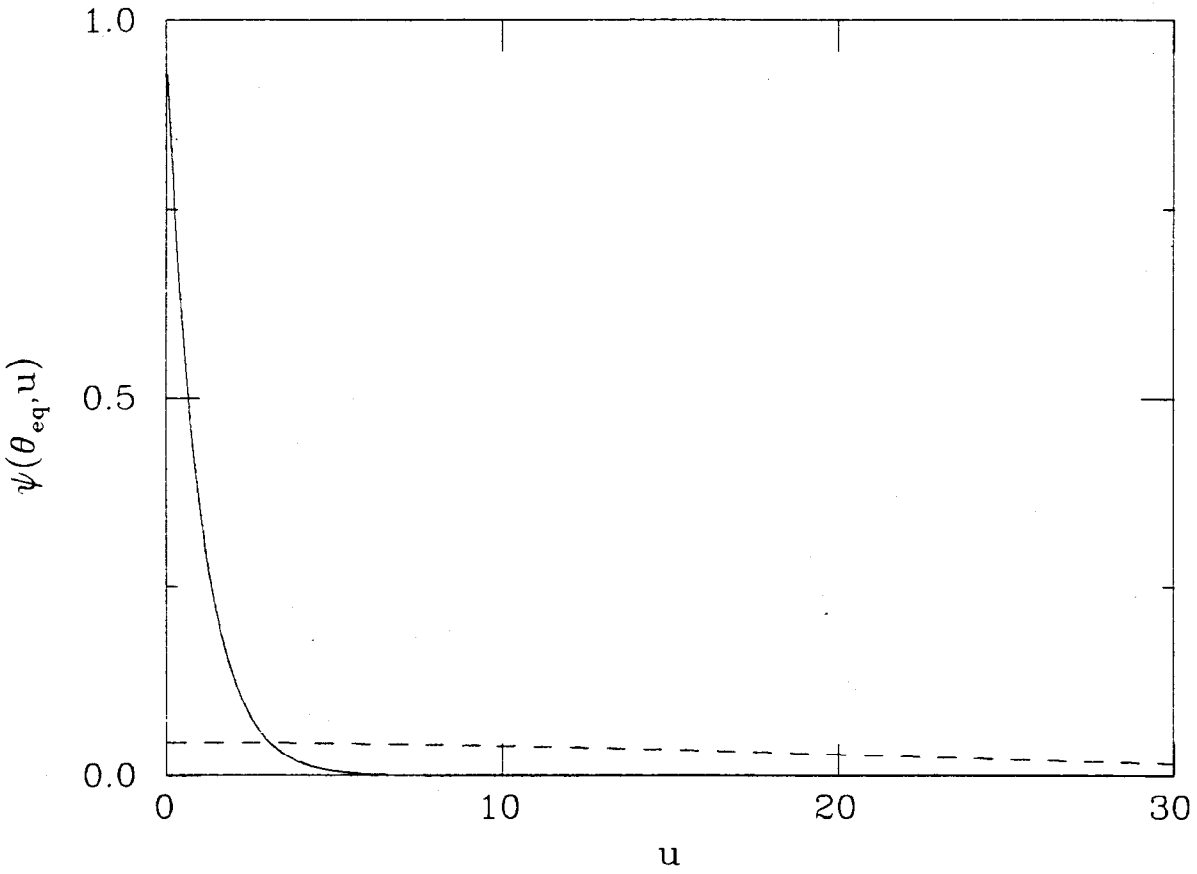

Fig. 13

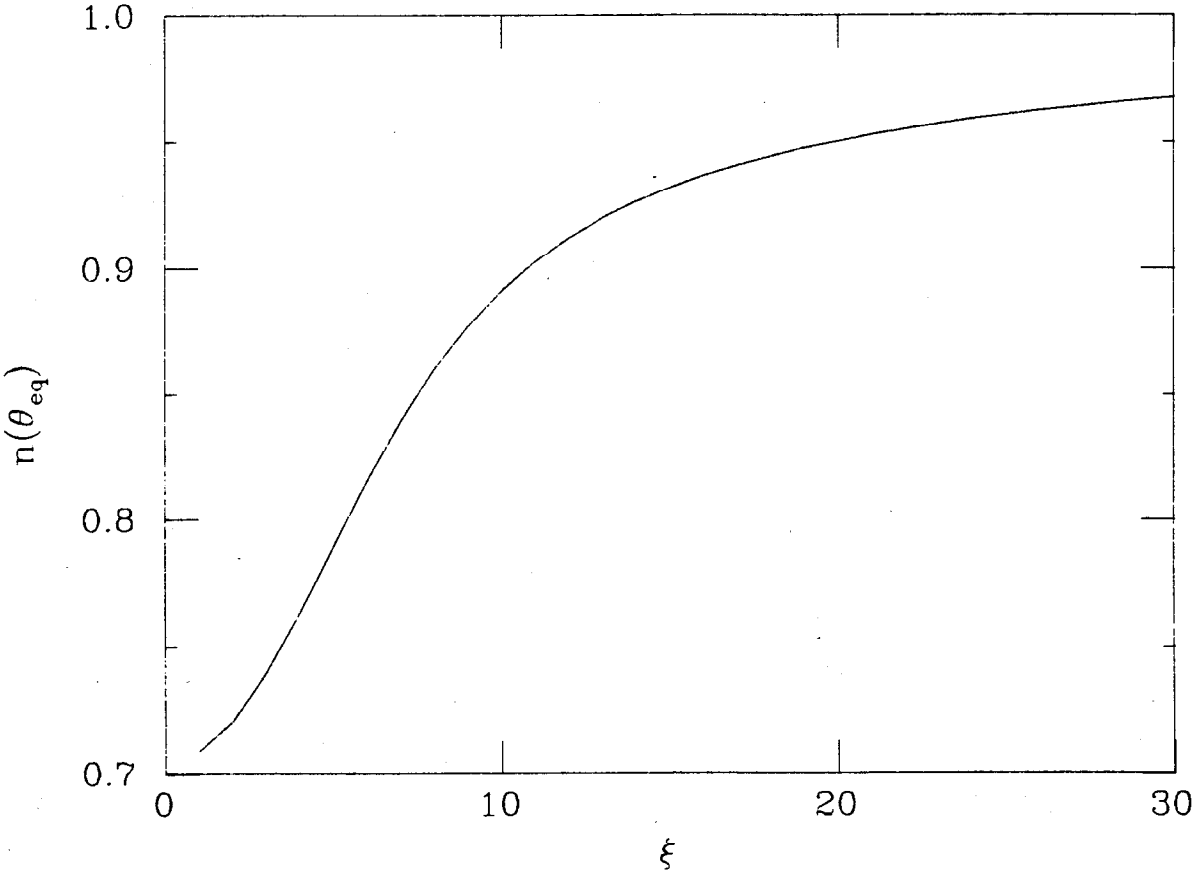

Fig. 14